Electronic Supplementary Material (ESI) for Dalton Transactions.
This journal is © The Royal Society of Chemistry 2014

Electronic Supplemental Information for:

An Unprecedented 3D POM-MOF based on (7, 8)-Connected Twin Wells-Dawson Clusters: Synthesis, Structure, Electrocatalytic and Photocatalytic Properties

Shaobin Li,[a] Li Zhang,[a] Kevin P. O'Halloran[b], Huiyuan Ma*[a] and Haijun Pang*[a]

[a]Key Laboratory of Green Chemical Engineering and Technology of College of Heilongjiang Province, College of Chemical and Environmental Engineering, Harbin University of Science and Technology, Harbin 150040.

[b]School of Science and Technology, Georgia Gwinnett College, Lawrenceville, GA 30043, USA.

CONTENTS

Section 1 Experimental Section

I. Materials and General Methods

The α-$K_6P_2W_{18}O_{62}\cdot 15H_2O$ was prepared according to the literature method.[1] All other reagents were purchased commercially and were used without further purification. Elemental analyses (C, H and N) were performed on a Perkin-Elmer 2400 CHN Elemental Analyzer, and that of Cu, W were carried out with a Leaman inductively coupled plasma (ICP) spectrometer. The FT-IR spectra were recorded from KBr pellets in the range of 4000–400 cm^{-1} with a Nicolet AVATAR FT-IR360 spectrometer. The powder X-ray diffraction (PXRD) data were collected on a Rigaku RINT 2000 diffractometer at room temperature. UV-vis absorption spectra were recorded on a 756 CRT UV-vis spectrophotometer.

II. Synthesis of 1

A mixture of α-$K_6P_2W_{18}O_{62}\cdot 15H_2O$ (0.35 g, 0.072 mmol), $Cu(NO_3)_2\cdot 3H_2O$ (0.15 g, 0.6 mmol), btb (0.072 g, 0.38 mmol) and triethylamine (0.2 mL) were dissolved in 15 mL of distilled water at room temperature. After the pH value of the mixture was adjusted to about 4.5 with 1.0 mol L^{-1} NaOH, the suspension was put into a Teflon-lined autoclave and kept under autogenous pressure at 170 °C for 5 days. After slow cooling to room temperature, blue rhombic block crystals of **1** were filtered, washed with distilled water and dried at room temperature. Yield: 47 % (based on W). The final pH value of the solution after the reaction is approximate to 4.0. Elemental analysis calc (%) for $C_{152}H_{266}O_{204}N_{114}P_6W_{54}Cu_{11}$: C 10.28, H 1.51, N 8.99, Cu 3.93, W 55.88 %; Found: C 10.42, H 1.42, N 9.18, Cu 4.11, W 56.33 %.

III. X-ray Crystallography

Single-crystal X-ray diffraction data collection of compound **1** was performed using a Bruker Smart Apex CCD diffractometer with Mo-*Ka* radiation (λ = 0.71073 Å) at 293 K. Absorption correction was applied by using the multi-scan program SADABS.[2] The structure was solved by the direct method, and non-hydrogen atoms were refined anisotropically by least-squares on F^2 using the SHELXTL program.[3] The hydrogen atoms of organic ligands were generated geometrically for **1**, while the hydrogen atoms of water molecules can not be found from the residual peaks and were directly included in the final molecular formula. Crystallographic data for the structures reported in this paper have been deposited in the Cambridge Crystallographic Data Center with CCDC Number: 1030489.

Reference

1 D. K.Lyon, W. K.Miller, T.Novet, P. J. Domaille, E. Evitt, D. C. Johnson and R. G. Finke, *J. Am. Chem. Soc.*, 1991, **113**, 7209.

2 G. M. Sheldrick, *SADABS 2.05*; University of Göttingen: Göttingen, Germany.

3 *SHELXTL 6.10*; Bruker Analytical Instrumentation: Madison, WI, 2000.

IV. Photocatalytic Experiments

Before conducting the photocatalytic experiments, the sample of compound **1** was full characterized by IR, XPS and PXRD (see details in the following section of Supplementary Physical Characterizations). The photocatalytic reactions were carried out at room temperature. The photodecomposition of methylene blue (MB) is evaluated under UV light irradiation through a typical process: 60 mg of powdered **1** was mixed together with 100 mL of a 1.0×10^{-5} mol/L (C_0) solution of MB. Then, the mixture was continuously stirred under UV irradiation from a 250 W high-pressure Hg lamp. At 0, 30, 60, 90, 120 and 150 min, an aliquot (3 mL) was taken from the beaker respectively, followed by several centrifugations to remove **1** and a clear solution was obtained for UV-vis analysis.

Section 2 Supplementary Structural Section

Table S1. Summary of the known POMOFs based on mixed-connected POM clusters.

No.	**Compounds**	**Coordination numbers**	**Coordination modes**	**References**
1	$[Ni_3(L^1)_5][PMo_{12}O_{40}]_2\cdot 14H_2O$	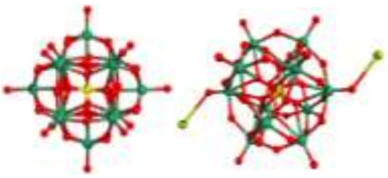	[0+2]	*Wang et al.*, ***Cryst. Growth Des.*** 2011, 11, 3456.
2	$[Cu(bbi)]_2[Cu_2(bbi)_2(\delta\text{-}Mo_8O_{26})_{0.5}]$ $[\alpha\text{-}Mo_8O_{26}]_{0.5}$	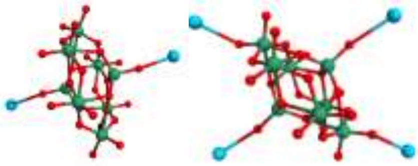	[2+4]	*Su and Wang et al.*, ***Inorg. Chem.***, 2008, 47, 529.
3	$[Cu_{12}(C_7H_{12}N_8S_2)_9(HSiW_{12}O_{40})_4]$ $\cdot 0.5H_2O$	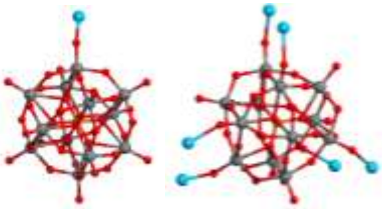	[1+6]	*Wang et al.*, ***Chem. Commun.***, 2010, 46, 6485.
4	$[Ag_8(btp)_4(H_2O)_2(HPW^{VI}_{10}W^{V}_{2}O^{40})_2]$ $\cdot H_2O$	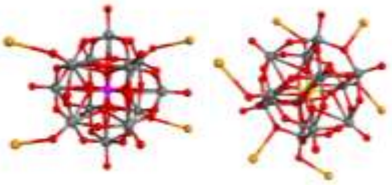	[4+6]	*Wang et al.*, ***CrystEngComm.***, 2013, 15, 4516.
5	$H_2[Cu_{11}(btb)_{19}(H_2O)_6(P_2W_{16}^{VI}W_2^{V}O_{62})_3]$ $\cdot 12H_2O$	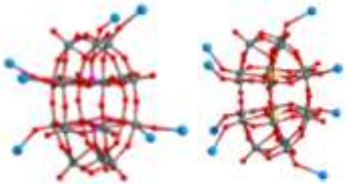	[7+8]	This work

Table S2 Crystal data and structure refinements for **1**.

Compound	**1**
Formula	$C_{152}H_{266}Cu_{11}N_{114}O_{204}P_6W_{54}$
Formula weight	17767.17
Crystal system	Monoclinic
Space group	*C2/c*
a/Å	48.819(5)
b/Å	21.863(5)
c/Å	36.741(5)
β/°	111.584(5)
V/Å^3	36465(10)
Z	4
D_{calcd}/g cm^{-3}	3.203
T/K	293(2)
μ/mm^{-1}	17.708
Refl. Measured	92134
Refl. Unique	32319
R_{int}	0.1076
GoF on F^2	0.998
R_1/wR_2 [$I \geq 2\sigma(I)$]	0.0604/0.1482

$R_1 = \sum \| F_o | - | F_c \| / \sum | F_o |$. $wR_2 = \sum[w(F_o^2 - F_c^2)^2]/\sum[w(F_o^2)^2]^{1/2}$

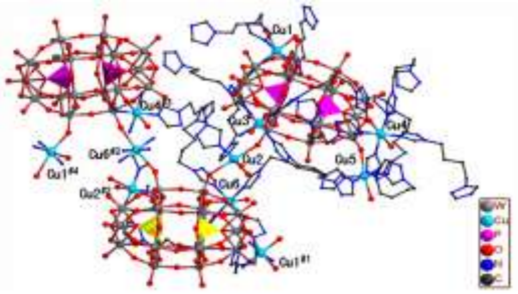

Fig. S1 View of the asymmetric unit of **1** and the coordination environments around the Cu atoms. All hydrogen atoms are omitted for clarity. (Symmetry code: #1, x, 1 + y, z; #2, 2 - x, y, 1.5 - z; #3, 1.5 - x, 0.5 - y, 1 - z; 4#, x, -y, 0.5 + z.).

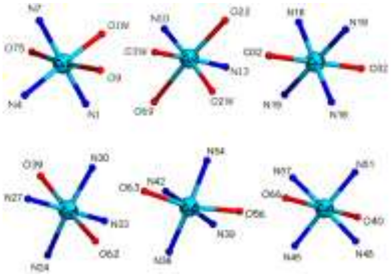

Fig. S2 The coordination environments of six crystallographically-independent Cu ions.

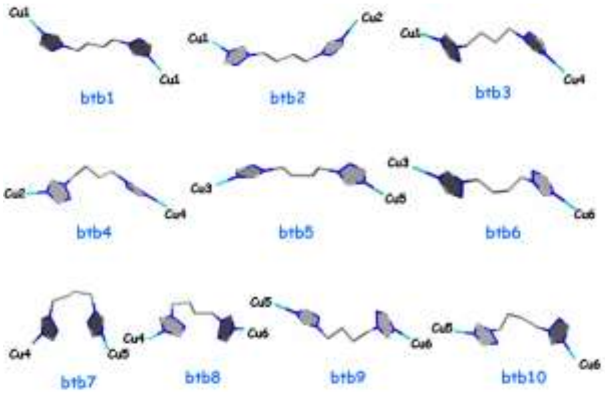

Fig. S3 The coordination environments of ten crystallographically-independent btb ligands.

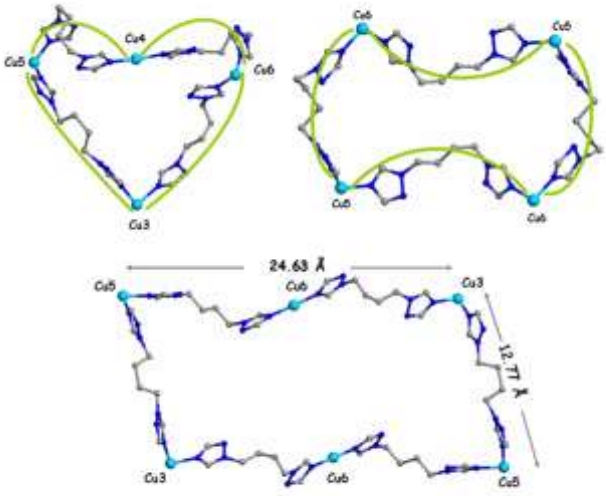

Fig. S4 The three kinds of macrocycles in **1**.

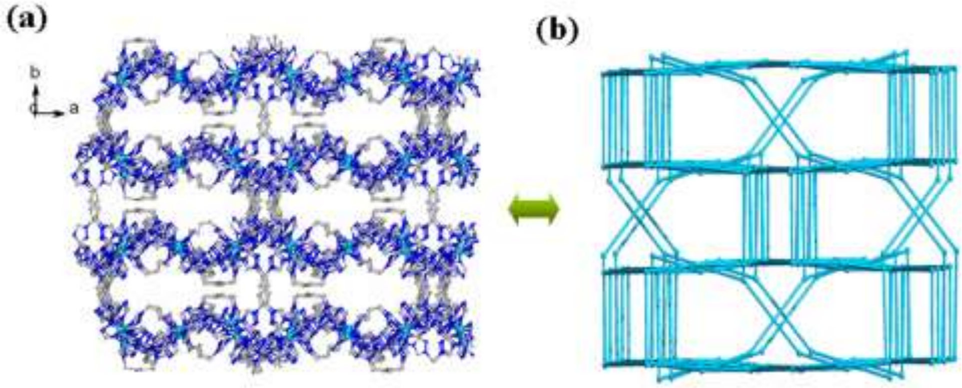

Fig. S5 (a) The organic-inorganic framework constructed by Cu ions and btb ligands, (b) topology of the 3D organic-inorganic framework.

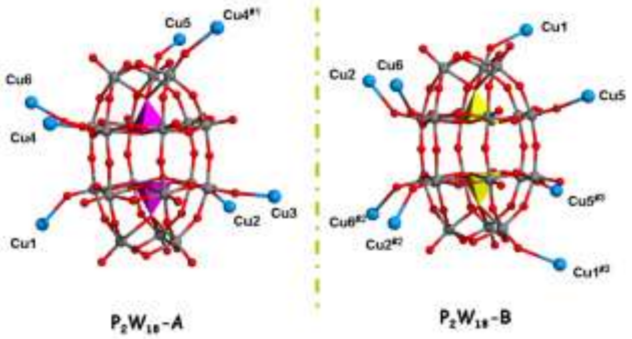

Fig. S6 View of the connection environment of two crystallographically-distinct P_2W_{18} clusters. (Symmetry code: #1, x, 1 + y, z; #2, 2 - x, y, 1.5 - z; #3, 1.5 - x, 0.5 - y, 1 - z.).

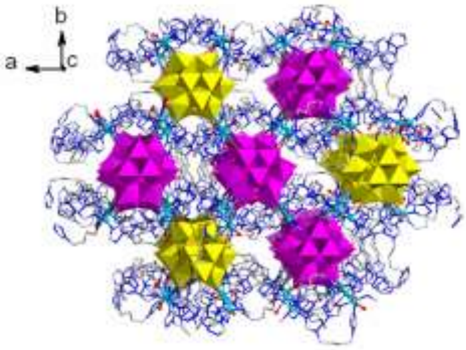

Fig. S7 View of the final structure of compound **1**.

Section 3 Supplementary Physical Characterizations

I. Analyses of BVS, XPS, IR, and TG measurements

BVS and XPS: Compound **1** was synthesized under hydrothermal conditions. All copper atoms in **1** are in the +II oxidation state, confirmed by their octahedral coordination environments, blue crystal color and BVS calculations.[4] The XPS spectrum of **1** shows two overlapping peaks at 35.17 eV and 37.26 eV (Fig. S8), which are attributed to W^{V} and W^{VI}, respectively.[5] All of these results are consistent with the structural analyses and charge balance. In the synthetic procedure of **1**, the W(VI) was partially reduced to W(V). The triethylamine is a necessary starting material for obtaining compound **1**, although it is not in the existence of final structure. The triethylamine in this reaction may have acted not only as a mineralization agent but also a reducing agent. Organic amine such as triethylamine, is a good candidate as reducing agent, which is easy to reduce the POMs to heteropoly blues anions especially under hydrothermal conditions.[6] In addition, for charge balance, since **1** was isolated from acidic aqueous solution, two protons are included in the formula of **1**, which is similar to the cases of $H\{Cu_2(\mu_2\text{-}OH)_2L\ [CrMo_6(OH)_6O_{18}]\}\cdot 4H_2O$ and $H_5[Ba_{10}(NMP)_{14}(H_2O)_8(V_{12}O_{33})_4Br]$.[7]

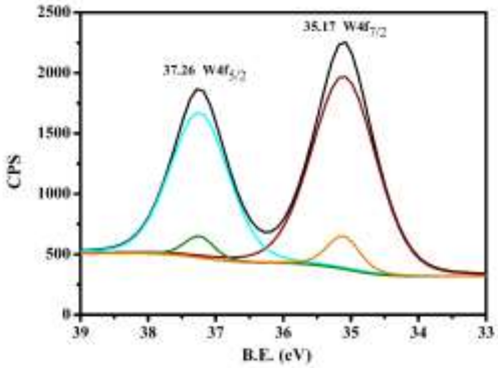

Fig. S8 The XPS spectrum of compound **1**.

IR: The IR spectrum exhibits the characteristic peaks at 1031, 973, 861 and 769 cm^{-1} in **1** (Fig. S9), which are attributed to ν(P-O), ν(W=Ot), ν_{as}(W–Ob–W) and ν_{as}(W–Oc–W), respectively. Compared to the typical Wells-Dawson type P_2W_{18} polyanion, compound **1** has similar peaks in the range of 750–1070 cm^{-1} except for slight shifts of peaks due to the interactions between the polyanions and the Cu(II) ions in the solid state, which indicates that the P_2W_{18} cluster in the title compound still retains the basic structure of Wells-Dawson P_2W_{18} polyanion.[8] Additionally, the characteristic peaks in the region 1628 to 1259 cm^{-1} could be ascribed to the characteristic peaks of btb ligands.[9]

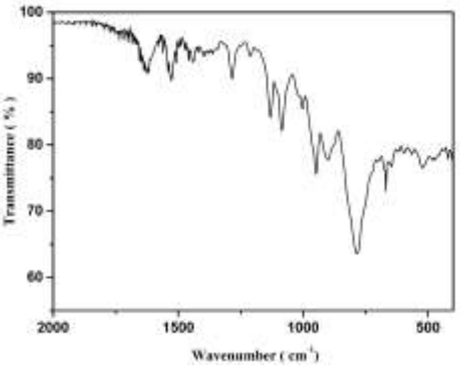

Fig. S9 The IR spectrum of compound **1**.

TG: The TG curve of **1** was performed in air to explore its thermal stability and the curve exhibits two weight loss steps in the range of 25 – 800 °C (Fig. S10). The first weight loss step of 3.55 % (calc. 3.13 %) below 100 °C corresponds to the loss of water molecules for compounds **1**. There is nearly no weight loss in the range of 100 – 320 °C, which verifies that due to the high connected structure, the POM-MOF in **1** is high stable even in *ca.* 320 °C. The second weight loss step of 31.91 % (calc. 32.84 %) occurred in the range of 325 – 550 °C is ascribed to the decomposition of organic molecules and collapse of P_2W_{18} clusters.. The whole weight loss of 35.46 % is in agreement with the calculated value 35.97 %, which also supports the chemical composition of **1**.

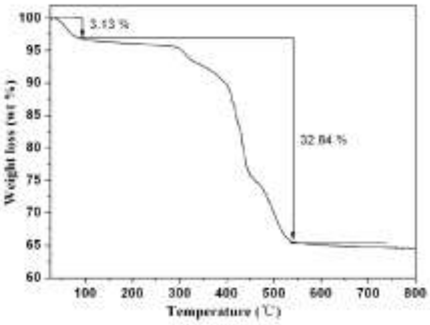

Fig. S10 The TG curve of compound **1**.

Reference

4 I. D. Brown and D. Altermatt, *Acta Crystallogr. Sect. B: Struct. Sci.*, 1985, **41**, 244.

5 Y. K. Lu, X. B. Cui, Y. Chen, J. N. Xu, Q. B. Zhang, Y. B. Liu, J. Q. Xu and T. G. Wang, *J. Solid State Chem.*, 2009, **182**, 2111.

6 (*a*) C. J. Zhang, H. J. Pang, Q. Tang, H. Y. Wang and Y. G. Chen, *Dalton Trans.*, 2010, **63**, 7993; (*b*) Y. Q. Lan, S. L. Li, X. L. Wang, K. Z. Shao, D. Y. Du, H. Y. Zang and Z. M. Su, *Inorg. Chem.*, 2008, **47**, 8179; (*c*) X. C. Huang, J. P. Zhang, Y. Y. Lin, X. L. Yu and X. M. Chen, *Chem. Commun.*, 2004, 1100.

7 (*a*) X. L. Wang, Z. H. Chang, H. Y. Lin, A. X. Tian, G. C. Liu and J. W. Zhang, *Dalton Trans.*, 2014, **43**, 12272; (*b*) K. Kastner, B. Puscher and C. Streb, *Chem. Commun.*, 2013, **49**, 140.

8 J. Q. Sha, J. Peng, Y. Q. Lan, Z. M. Su, H. J. Pang, A. X. Tian, P. P. Zhang and M. Zhu, *Inorg. Chem.*, 2008, **47**, 5145.

9 A. X. Tian, J. Ying, J. Peng, J. Q. Sha, Z. G. Han, J. F. Ma, Z. M. Su, N. H. Hu and H. Q. Jia, *Inorg. Chem.*, 2008, **47**, 3274.

II. Equations of photocatalytic mechanisms

$[P_2W^{V}_2W^{VI}_{16}O_{62}]^{8-} + h\nu \rightarrow [{}^*P_2W^{V}_2W^{VI}_{16}O_{62}]^{8-}$ (1)

$[{}^*P_2W^{V}_2W^{VI}_{16}O_{62}]^{8-} + H_2O \rightarrow [P_2W^{V}_2W^{VI}_{16}O_{62}]^{9-} + H^+ + OH^{\cdot}$ (2)

$[P_2W^{V}_2W^{VI}_{16}O_{62}]^{9-} + O_2 \rightarrow [{}^*P_2W^{V}_2W^{VI}_{16}O_{62}]^{8-} + O_2^{-}$ (3)

$MB + h\nu \rightarrow {}^*MB$ (4)

$^*MB + OH^{\cdot} + O_2^{-} \rightarrow$ intermediate products → degradation (5)

III. Additional figures for photocatalytic experiments

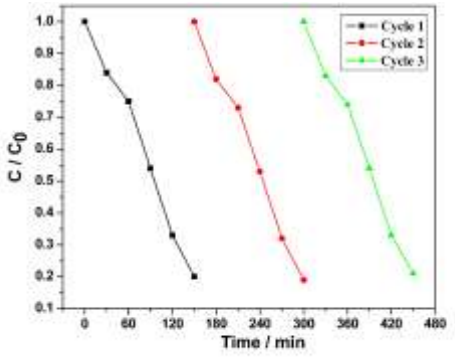

Fig. S11 Three runs of the MB degradation test by compound **1**.

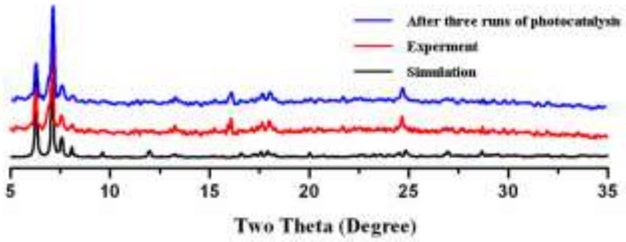

Fig. S12 The simulated (black), experimental (red) and after three runs of photocatalysis (blue) PXRD patterns of compound **1**.

IV. The electrocatalytic property of 1

The POMs possess the ability of undergoing reversible multi-electron redox processes, which makes them very attractive in chemically-modified electrode and the electrocatalytic study.[10] Due to the title compounds are insoluble in water and common organic solvents. Thus, the bulk-modified carbon paste electrode (CPE) becomes the optimal choice to study the electrochemical properties, which is inexpensive, easy to prepare and handle.[11]

The cyclic voltammetric behavior for **1**-CPE (carbon paste electrode) was studied in 1 M H_2SO_4 solution (Fig. S13). In the potential range of -0.7 to 0.4 V, there exist three redox peaks with half-wave potentials E1/2 at -0.07 (II-II’), -0.26 (III-III’) and -0.55 V (IV-IV’), which can be ascribed to redox processes of tungstate in **1**. In addition, there is one irreversible anodic peak (I) at +0.19 V, which is assigned to the oxidation of copper.[12] As shown in the insert of Fig. S13, when the scan rates are varied from 0.1 to 0.5 $V{\cdot}s^{-1}$, the peak potentials change gradually: the cathodic peak potentials shift toward the negative direction and the corresponding anodic peak potentials to the positive direction with increasing scan rates. The peak currents are proportional to the scan rate, which indicate that the redox processes are surface-controlled.[13]

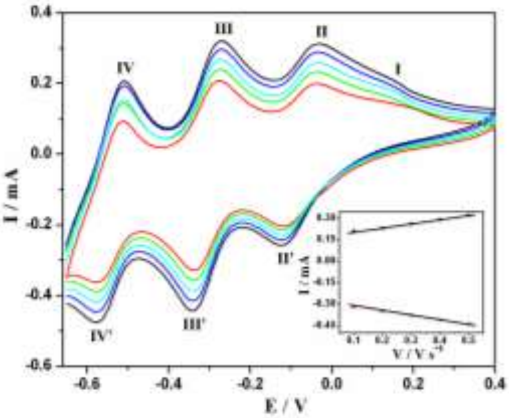

Fig. S13 Cyclic voltammograms for **1**-CPE in 1 M H_2SO_4 solution at different scan rates (from inner to outer): 0.1, 0.2, 0.3, 0.4 and 0.5 V s^{-1}.The inset shows plots of the anodic and the cathodic peak currents for III againt scan rates.

The POMs have been exploited extensively in electrocatalytic reactions and further applications such as biosensors and fuel cells.[14] Herein, the reduction of iodated (IO_3^-) and nitrite (NO_2^-) were chosen as test reaction to study the electrocatalytic activity of **1**. As shown in Fig. 5, it displays good electrocatalytic activity toward the reduction of IO_3^- and NO_2^- in 1 M H_2SO_4 solution. With the addition of IO_3^- and NO_2^-, the cathodic peak IV substantially increased, while the corresponding anodic peak currents decreased. The inset of Fig. S14 a and b show the relationship between the fourth cathodic current and concentration of IO_3^- and NO_2^-. The electrocatalytic efficiency of **1**-CPE (based on a rough calculation using CAT formula)[15] toward the reduction of IO_3^- and NO_2^- were *ca.* 85 % and 97 % at 1M H_2SO_4 containing 30 mM hydrogen peroxide and nitrite, which suggests that **1** has potential applications in detection of hydrogen peroxide and nitrite.

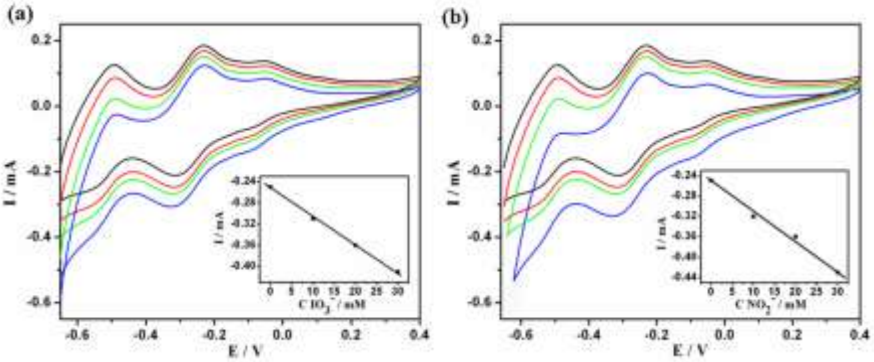

Fig. S14 Reduction of IO_3^- (a) and NO_2^- (b) at **1**-CPE in 1 M H_2SO_4 solution containing IO_3^- and NO_2^- in various concentrations (from inner to outer): 0, 10, 20, 30 mM. The inset shows a linear dependence of the cathodic catalytic current of wave IV with IO_3^- and NO_2^- concentration, respectively.

Reference

10 X. D. Xi, G. Wang, B.F. Liu and S.J. Dong, *Electrochim. Acta*., 1995, **40**, 1025.

11 Z. G. Han, Y. L. Zhao, J. Peng, Y. H. Feng, J. N. Yin and Q. Liu, *Electroanalysis*. 2005, **17**, 1097.

12 (*a*) A. X. Tian, J. Ying, J. Peng, J. Q. Sha, H. J. Pang, P. P. Zhang, Y. Chen, M. Zhu, Z. M. Su, *Inorg. Chem*., 2009, **48**, 100; (*b*) C. D. Zhang, S. X. Liu, C. Y. Sun, F. J. Ma and Z. M. Su, *Cryst Growth Des*., 2009, **9**, 3655.

13 X. L. Wang, Q. Gao, A. X. Tian, H. L. Hu and G. C. Liu, *J. Solid State Chem.*, 2012, **187**, 219.

14 (*a*) B. Keita, P.D. Oliveira, L. Nadjo and U. Kortz, *Chem. Eur. J.*, 2007, **13**, 5480; (*b*) C. Pichon, P. Mialane, A. Dolbecq, J. Marrot, E. RiviLre, B. Keita, L. Nadjo and F. Secheresse, *Inorg. Chem*., 2007, **46**, 5292.

15 B. Keita, A. Belhouari, L. Nadjo and R. Contant, *J. Electroanal, Chem.*, 1995, **381**, 243.